Magnetic Properties of Mixed Ligand NiII2 and NiII4 Complexes Composed of Macrocyclic Hexaamine-Dithiophenolato and Bridging Tetrazolato Ligands

Berthold Kersting

Zeitschrift für Anorganische und Allgemeine Chemie

Magnetic Properties of Mixed Ligand NiII2 and NiII4 Complexes Composed of Macrocyclic Hexaamine-Dithiophenolato and Bridging Tetrazolato Ligands

Journal:	*Zeitschrift für Anorganische und Allgemeine Chemie*
Manuscript ID:	zaac.201000087.R1
Wiley - Manuscript type:	Article
Date Submitted by the Author:	29-Apr-2010
Complete List of Authors:	Kersting, Berthold; Universitaet Leipzig, Institut fÂ r Anorganische Chemie
Keywords:	Nickel Complexes, Coordination Chemistry, Tetrazolato Complexes, Magnetic Properties
Note: The following files were submitted by the author for peer review, but cannot be converted to PDF. You must view these files (e.g. movies) online.	
Figure2.cdx Scheme1.cdx Scheme2.cdx Scheme3.cdx	

Magnetic Properties of Mixed Ligand Ni^{II}_2 and Ni^{II}_4 Complexes Composed of Macrocyclic Hexaamine-Dithiophenolato and Bridging Tetrazolato Ligands

Jochen Lach,[a] Sergei V. Voitekhovich,[b] Vasile Lozan,[c] Pavel N. Gaponik,[b] Oleg A. Ivashkevich,[b] Jörg Lincke,[a] Daniel Lässig,[a] and Berthold Kersting[a*]

[a]Institut für Anorganische Chemie, Universität Leipzig, Johannisallee 29, D-04103 Leipzig, Germany

[b]Research Institute for Physical Chemical Problems, Belarusian State University, Leningradskaya 14, 220030 Minsk, Belarus

[c]Laboratory of Coordination Chemistry, Institute of Chemistry, Academy of Sciences of Moldova, Academiei str. 3, MD-2028, Chisinau, Republic Moldova

Reprint requests to Prof. Dr. Berthold Kersting, FAX +49 341 973 6199.

E-mail: b.kersting@uni-leipzig.de

Abstract. The magnetic properties of the dinuclear and tetranuclear nickel(II) tetrazolato complexes $[Ni_2L(RCN_4)][BPh_4]$ (R = H (**4**), Me (**5**), Ph (**6**)) and $[(Ni_2L)_2(1,4\text{-}(CN_4)_2\text{-}C_6H_4)][BPh_4]_2$ (**7**), where $(L)^{2-}$ represents a 24-membered macrocyclic N_6S_2 supporting ligand, are reported. Analysis of temperature-dependent magnetic susceptibility measurements over the temperature range from 2 to 300 K reveals the presence of weak ferromagnetic exchange interactions between the Ni^{II} ions in the binuclear $[Ni_2L(\mu\text{-}L')]^+$ subunits with values for the magnetic exchange coupling constants J_1 of 13.5 cm^{-1} for **4**, 20.0 cm^{-1} for **5**, 19.2 cm^{-1} for **6**, and 15.2 cm^{-1} for **7** ($\mathbf{H} = -2J\mathbf{S}_1\mathbf{S}_2$). The exchange coupling J_2 across the bistetrazolato bridge in **7** is less than 0.1 cm^{-1} suggesting that no significant

interdimer coupling occurs in this compound. The synthesis and crystal structure of the new complex **7**·2MeCN is also reported.

Key words: Nickel Complexes, Coordination Chemistry, Tetrazolato Complexes, Magnetic Properties

Introduction

The five-membered N-heterocycles pyrazolate [1] and tetrazolate [2] have a rich coordination chemistry due to a number of different coordination modes. To establish if substantial structural and chemical analogy exists between pyrazolato and tetrazolato complexes, we are preparing isostructural complexes of the general form $[Ni_2L(\mu\text{-}L')]^+$ (L' = $RC_3H_2N_2^-$ or RCN_4^-) [3–5]. The macrocyclic hexaamine-dithiophenolato ligand L^{2-} [6] enforces accommodation of the pyrazolato and tetrazolato ligands in analogous, that is, symmetric bridging modes (Scheme 1).

<< Scheme 1 here >>

Scheme 1. Coordination modes of pyrazolato and tetrazolato ligands in dinuclear $[Ni_2L(L')]^+$ complexes (supporting ligand L^{2-} omitted for clarity).

The X-ray crystal structures of the pyrazolato complexes $[Ni_2L(C_3H_3N_2)]^+$ (**1**) [3], $[(Ni_2L)_2(4,4'\text{-}(C_3H_2N_2)_2)]^{2+}$ (**2**) [4], $[(Ni_2L)_2(1,4\text{-}(C_3H_2N_2)_2C_6H_4)]^{2+}$ (**3**) [4], and the tetrazolato complexes $[Ni_2L(HCN_4)]^+$ (**4**), $[Ni_2L(MeCN_4)]^+$ (**5**), and $[Ni_2L(PhCN_4)]^+$ (**6**) have already been reported [5]. It was established that tetrazolato ligands RCN_4^- interact less strongly with

the $[Ni_2L]^{2+}$ fragment than pyrazolato ligands $RC_3H_2N_2^-$ [5], as can be seen from the Ni–$N_{coligand}$ bond length noted in Table 2.

In this work we describe the synthesis, characterization and X-ray single-crystal structure determination of the new tetranuclear Ni^{II}_4 complex $[(Ni^{II}_2L)_2(1,4\text{-}(CN_4)_2\text{-}C_6H_4)][BPh_4]_2$ (**7**) and discuss the structural differences between **3** and **7**. The results of temperature-dependent magnetic susceptibility measurements on **4**, **5**, **6**, and **7** are also described.

Results and Discussion

Scheme 2 shows the synthesized compounds and their labels. The dinuclear Ni^{II} complexes $[Ni_2L(HCN_4)][BPh_4]$ (**4**), $[Ni_2L(MeCN_4)][BPh_4]$ (**5**) and $[Ni_2L(PhCN_4)][BPh_4]$ (**6**) bearing tetrazolato (HCN_4^-), 5-Me-tetrazolato ($MeCN_4^-$), or 5-Ph-tetrazolato ($PhCN_4^-$) coligands respectively, were prepared as described in the literature [5]. The tetrazole 5,5'-(1,4-phenylene)bis-1*H*-tetrazole (H_2pbtz), necessary for the preparation of **7**, was synthesized from 1,4-dicyanobenzene according to a literature procedure [7]. The tetranuclear complex $[Ni^{II}_2L(1,4\text{-}(CN_4)_2\text{-}C_6H_4)][BPh_4]_2$ (**7**) was prepared by a substitution reaction between the chlorido complex $[Ni^{II}_2L(\mu\text{-}Cl)][ClO_4]$ [6] and triethylammonium 5,5'-(1,4-phenylene)bis-1*H*-tetrazolato (prepared *in situ* from the corresponding bistetrazole and triethylamine) in a 1:2 molar ratio, followed by precipitation with $LiClO_4$ and subsequent metathesis with $NaBPh_4$ in 64 % yield as outlined in Scheme 2. The linking of the two $[Ni^{II}_2L]^{2+}$ fragments by the bistetrazolato ligand is a clean and facile step driven forward by the low solubility of the product. A similar approach was used to prepare the tetranuclear complex **3** [5].

<< Scheme 2 here >>

Scheme 2. Structures and synthesis of complexes **3** – **7**.

All compounds gave satisfactory elemental analyses and were characterized by appropriate spectroscopic methods (IR, UV/Vis and ESI-MS), as well as by X-ray single-crystal structure analysis. The tetraphenylborate salt **7** is an air-stable solid that is soluble in aprotic solvents such as dimethylformamide, dichloromethane, and acetonitrile, but virtually insoluble in methanol, ethanol and water. The electrospray ionization mass spectrum (ESI-MS, positive mode) of a dilute CH_2Cl_2 solution of **7** exhibits a molecular ion peak with the correct isotopic distribution for the dication $\mathbf{7}^{2+}$ (m/z = 891.36). Two prominent absorption bands are seen in the UV/Vis spectrum of **7** in CH_2Cl_2, as in the tetrazolato-bridged Ni_2 complexes **4** – **6**, at 615 and 1133 nm [5]. These are assigned to the spin-allowed $^3A_{2g} \rightarrow {}^3T_{1g}$ (ν_2) and $^3A_{2g} \rightarrow {}^3T_{2g}$ (ν_1) transitions of a nickel(II) (S = 1) ion (in O_h symmetry for simplicity) [8]. The observed values closely compare with those of **4** – **6** indicative of pseudo-octahedral $N_3S_2N^{tetrazolate}$ coordination environments around the metal atoms. The intensities of ν_1 and ν_2 are approximately twice as large as those of **4** – **6**, which is in good agreement with the formulation of compound **7** as a 2:1 complex. The salt **7** reveals also four well-resolved UV bands at 231, 270, 336, and 391 nm, the former three of which are attributable to the π-π* transitions within the thiophenolato units of the $[Ni_2L]^{2+}$ fragments. The band at 391 nm can be attributed to a thiophenolate → Ni^{II} charge transfer absorption [9]. All these findings strongly indicate that the tetranuclear complex in **7** remains its integrity in the solution state.

Description of the Crystal Structures of 7·2MeCN and 7·CH_2Cl_2

Single-crystals suitable for X-ray structure analysis could be obtained by two different methods. In a first attempt crystals were grown by slow diffusion of methanol into a solution of **7** in dichloromethane. Unfortunately those crystals gave unsatisfying R-values because of heavily disordered CH_2Cl_2 in the crystal structure, making it necessary to use the SQUEEZE routine of PLATON [10]. Slow evaporation of a 1:1 acetonitrile/ethanol solution of **7** yielded single-crystals of **7**·2MeCN giving much better R-values. Both crystal structures are composed of tetranuclear $[(Ni_2L)_2(1,4\text{-}(CN_4)_2C_6H_4)]^{2+}$ dications, tetraphenylborate anions, and acetonitrile (or dichloromethane) solvent molecules respectively. The structure of **7**·2MeCN is representative and will be discussed.

An ORTEP plot of the structure of the centrosymmetric dication of **7** is depicted in Figure 1. Selected bond lengths and angles are summarized in Table 1. The metrical data for the corresponding bispyrazolato complex $[(Ni_2L)_2(1,4\text{-}(C_3H_2N_2)_2C_6H_4)]^{2+}$ (**3**) [4] are included for comparison.

<< Figure 1 here >>

Figure 1. Left: Van der Waals plot of the $[(Ni_2L)_2(1,4\text{-}(CN_4)_2C_6H_4)]^{2+}$ dication in crystals of **7**·2MeCN. Right: ORTEP representation of the core structure of the dication with the atom labeling scheme. Ellipsoids are represented at the 50 % probability level. Symmetry code used to generate equivalent atoms: *–x*, *–y*, 2*–z* (').

The bistetrazolate unit acts as a tetradentate bridging ligand joining two dinuclear $[Ni^{II}_2L]^{2+}$ fragments through the ring nitrogen atoms N(7) and N(9). The $[Ni_2L]^{2+}$ subunits in **3** and **7** are structurally very similar, and the Ni–N and Ni–S distances lie within very narrow ranges (Table 1). The Ni···Ni distance in **7** is 3.442(1) Å, which is very similar to that in **3** and other dinuclear nickel complexes with bridging tetrazolates [5]. The $Ni–N_{tetrazolato}$ bond lengths reveal no anomalies and are comparable to those in **3**. Each Ni^{II} atom is surrounded in a

highly distorted octahedral fashion by two sulfur atoms and three nitrogen atoms from the supporting ligand L^{2-}, and one nitrogen atom from the tetrazolato group.

Table 1. Selected bond lengths [Å] and angles [°] in **7**·2MeCN, **7**·CH_2Cl_2 and **3**·6MeCN·$2H_2O$ [2].

	7·2MeCN	**7**·CH_2Cl_2	**3**·6MeCN·$2H_2O$
N(7)–N(9)[a]	1.349(5)	1.321(3)	1.354(3)
Ni(1)–N(7)	2.078(4)	2.052(2)	2.065(2)
Ni(1)–N(1)	2.335(5)	2.270(2)	2.276(2)
Ni(1)–N(2)	2.147(4)	2.149(2)	2.186(2)
Ni(1)–N(3)	2.218(5)	2.273(2)	2.279(2)
Ni(1)–S(1)	2.528(2)	2.4537(6)	2.4692(5)
Ni(1)–S(2)	2.477(2)	2.5143(7)	2.4878(5)
Ni(2)–N(9)	2.048(4)	2.083(2)	2.091(2)
Ni(2)–N(4)	2.256(4)	2.271(2)	2.247(2)
Ni(2)–N(5)	2.160(4)	2.157(2)	2.236(2)
Ni(2)–N(6)	2.315(4)	2.262(2)	2.300(2)
Ni(2)–S(1)	2.545(2)	2.4642(7)	2.3983(5)
Ni(2)–S(2)	2.449(2)	2.4964(6)	2.4967(5)
Ni–N	2.195(4)	1,907(2)	2.210(2)
Ni–S	2.500(2)	2.4822(7)	2.4630(5)
Ni···Ni	3.442(1)	3.4253(1)	3.349(1)
Ni-Ni^{cent}/Ni-Ni^{cent}[b]	13.261(8)	13.3037(7)	14.040(1)
N-M-N_{cis}[c]	88.8(2)	88.83(8)	90.69(6)
N-M-N_{trans}[c]	176.1(2)	176.30(9)	177.04(6)
S-M-N_{cis}[c]	91.1(1)	91.09(6)	91.06(5)
S-M-N_{trans}[c]	170.7(1)	170.47(7)	170.22(5)
S-M-S[c]	80.72(5)	80.42(2)	80.46(2)
M-S-M[c]	87.03(5)	87.27(2)	85.68(2)

[a] N(9) corresponds to N(8) in **3**.
[b] Distance between center of the Ni···Ni axes of the Ni_2 units.
[c] Average values.

The major structural difference between **3** and **7** concerns the conformations of the tetradentate coligands (Figure 2). In **3**, the Ni_2-heterocycle planes are coplanar with each

other, and the central aromatic ring is twisted out of this plane, the dihedral angle being τ = 23.8(2)°. In **7**·2MeCN, the Ni_2N_2 planes are slightly folded with respect to the tetrazolato plane (folding angle = 173.4(2)°). The twisting angle between the central aromatic ring and the tetrazolato planes is smaller at 12.7(6)°. The corresponding data for **7**·CH_2Cl_2 are 178.0(1)° and 5.7(3)°. In contrast to **3**, there are also two short intramolecular C···C distances between the *t*Bu methyl groups and the aromatic ring, (d(C^{tBuMe} centroid phenyl ring): 3.634 Å), indicative of CH···π interactions [11].

<< Figure 2 here >>

Figure 2. Mutual orientation of the Ni_2tetrazolato and Ni_2pyrazolato planes in **7**·2MeCN, **7**·CH_2Cl_2 and **3**·6MeCN·$2H_2O$, respectively.

<< Figure 3_left and Figure 3_right here >>

Figure 3. Packing of the molecules in **7**·CH_2Cl_2 (left) and **7**·2MeCN (right). View along the *a* axis. Hydrogen atoms, solvent molecules and counter ions are omitted for clarity.

Figure 3 presents the packing of the molecules in the structures of **7**·CH_2Cl_2 and **7**·2MeCN. As can be seen, there are no significant intermolecular interactions between the Ni_4 complexes. The shortest intermolecular Ni···Ni distance is at 8.460(1) Å. The distance between the center of the Ni···Ni axes of the binuclear subunits amounts to 13.261(1) Å [12].

The N–N and N–C distances of the tetrazolato ligands in **7** differ significantly from the corresponding distances of the free 5,5'-(1,4-phenylene)bis-1*H*-tetrazole [13] and non-

coordinated 5,5'-(1,4-phenylene)bis-1*H*-tetrazolate anion [14]. Particularly affected are the N(7)–N(9) bonds. Thus, for bistetrazole and bistetrazolate these bonds lengths are 1.298(2) Å and 1.295(1) Å, much shorter than 1.354(3) Å in **3** or 1.349(5) Å in **7**. Similar differences were also observed for the set of tetrazolato complexes, **4** – **6** [5] showing N–N distances of 1.367(3), 1.331(3) and 1.353(5) Å.

Magnetic Properties

For the complexes **4** – **6**, and **7**·2MeCN temperature dependent magnetic susceptibility measurements were carried out using a MPMS 7XL SQUID (Quantum Design) magnetometer to investigate whether magnetic exchange interactions are present in the complexes. The susceptibility data have been recorded for dry, powdered samples between 2 and 300 K in an applied external field of 1.0 T. The temperature dependence of the effective magnetic moment for the four complexes is shown in Figure 4.

<< Figure 4 here >>

Figure 4. Temperature dependence of μ_{eff} for **4** (open stars), **5** (open squares), **6** (open triangles), and **7** (open circles). The solid lines represent the best theoretical fits to equations 1 and 2 (see text). Experimental and calculated values are provided as Supporting Information.

The complexes **4** – **6** show similar magnetic properties. At room temperature, the respective values of μ_{eff} are 4.71 μ_B, 4.67 μ_B and 4.67 μ_B per dinuclear complex. With decreasing temperature the μ_{eff} values increase steadily to maximum values of 5.60 μ_B (14 K), 5.35 μ_B (22 K) and 5.30 μ_B (20 K) for **4**, **5** and **6**, respectively. On lowering the temperature these

values decrease again to 4.98 μ_B, 4.18 μ_B and 4.35 μ_B at 2 K. This presumably occurs due to saturation effects or the zero-field splitting of nickel(II). For the tetranuclear complex **7** a slightly different behavior is observed. Here μ_B first increases from 6.54 μ_B at 300 K to a maximum value of 7.65 μ_B at 18 K and then again rapidly decreases to 5.62 μ_B at 2 K. The abrupt decrease in μ_B below 18 K is again presumably due to zero-field splitting of Ni^{II}. Although μ_{eff} at 18 K is smaller than the expected spin-only value of 9.84 μ_B for a $S_T = 4$ ground-state ($S_i = 1$, $g_i = 2.20$), it still is larger than 6.22 μ_B, a value which would be expected for four noninteracting Ni^{II} ions. This finding very much compares to what is observed for the structurally similar dipyrazolato complex $[(L^2Ni)_2(bpz)[BPh_4]_2]$ (**2**) [4, 15], where also no significant interdimer exchange coupling occurs. In conclusion it can be said that weak ferromagnetic exchange interaction can be noted within the dinuclear subunits, but virtually no interaction across the bistetrazolato bridge is seen.

The magnitude of the exchange interactions was determined by least-squares fitting of the experimental magnetic susceptibility data to the appropriate spin Hamiltonian equation 1 or 2 including the isotropic HDvV exchange, the single-ion Zero-field splitting and the single-ion Zeeman interactions using a full-matrix diagonalization approach [16].

$$H = -2J\hat{S}_1\hat{S}_2 + \sum_{i=1}^{2}\left[D_i(\hat{S}_{zi}^2 - \tfrac{1}{3}\hat{S}_i(\hat{S}_i+1)) + g_i\mu_B S_{i\tau}B_\tau\right] \quad (\tau = x, y, z) \quad (1)$$

$$H = -2J_1(\hat{S}_1\cdot\hat{S}_2 + \hat{S}_3\cdot\hat{S}_4) - 2J_2(\hat{S}_1\cdot\hat{S}_4 + \hat{S}_2\cdot\hat{S}_3) + \sum_{i=1}^{4}\left[D_i(\hat{S}_{zi}^2 - \tfrac{1}{3}\hat{S}_i(\hat{S}_i+1)) + g_i\mu_B S_{i\tau}B_\tau\right] \quad (\tau = x, y, z) \quad (2)$$

The experimental data of the binuclear compounds **4** – **6** were fitted to equation 1 over the temperature range 2 – 300 K, assuming identical D and g-values for the two Ni^{II} ions in each one of the complexes. The data are listed in Table 2 along with selected structural data. The data of the pyrazolato complex **2** are included for comparison. For the afore-mentioned complexes **4** – **6** J_1 was determined to be +13.5 cm^{-1}, +19.9 cm^{-1} and +19.2 cm^{-1}. The g-

values also show a very narrow distribution, namely 2.28, 2.20 and 2.17. *D*-values were also determined and all of them lie well below 10 cm^{-1} (Table 2). Although the inclusion of the *D* parameter improves the fit dramatically, *J* values are unaffected by its inclusion. Nonetheless the derived *D* values should be seen rather indicative. The finding that the J_1, *g* and *D* values are very similar corroborates nicely with the fact that the complexes **4** – **6** are structurally very similar (Table 2).

Scheme 3 illustrates the exchange coupling pathways used to model the susceptibility data of the tetranuclear complex **7**. In this model the exchange interaction between the Ni^{II} ions within a binuclear subunit are represented by J_1, whereas J_2 describes the interdimer interaction across the bistetrazolate bridge.

<< Scheme 3 here >>

Scheme 3. Magnetic exchange pathways used for simulation of the magnetic susceptibility data of the tetranuclear complex **7** (left) and the dinuclear complexes **4** – **6** (right).

The zero-field-splitting parameters *D* and the *g*-values were considered to be identical for all four Ni^{II} ions. Fitting the experimental data over the full temperature range led to J_1 = +15.2 cm^{-1}, J_2 = +0.1 cm^{-1}, *g* = 2.21 and *D* =+10.80 cm^{-1}. The low-temperature fit was significantly improved by the inclusion of the *D* parameter, but one should bear in mind that, since temperature-dependent magnetic susceptibility measurements are not very appropriate for the determination of *D*-values, the latter should be taken rather indicative than definite. In addition, temperature dependent magnetic susceptibility measurement are not very appropriate for the determination of the sign of *D* [17]. However, the theoretical fit reveals

that besides the expected exchange couplings in the binuclear subunits, no significant coupling (J_2 = +0.1 cm^{-1}) across the tetrazolate bridge occurs.

Table 2. Magnetic parameters J_1 [cm^{-1}], J_2 [cm^{-1}], g and |D| [cm^{-1}] for **2** and **4**-**7** and selected structural data.

	2	**4**	**5**	**6**[a]	**7**[b]
J_1[cm^{-1}]	+24.0	+13.5	+20.0	+19.2	+15.2
J_2[cm^{-1}]	<0.1	–	–	–	+0.1
g [c]	2.19	2.28	2.20	2.17	2.21
|D| [cm^{-1}] [c]	4.82	0.98	8.10	5.85	10.80
Ni···Ni [Å]	3.373(1)	3.455(1)	3.425(1)	3.447(1)	3.4253(1)
S-Ni-S [°][d]	82.10(2)	79.79(2)	80.30(3)	79.74(4)	80.42(2)
Ni-S-Ni [°][d]	85.53(2)	88.03(2)	87.12(3)	87.92(4)	87.27(2)
N(7)–N(9) [Å]	1.368(2)	1.367(3)	1.331(3)	1.353(5)	1.321(3)
Ni–$N_{coligand}$[d]	2.021(2)	2.080(2)	2.067(2)	2.061(3)	2.063(4)

[a] There are two crystallographically independent molecules A and B in the asymmetric unit. The second value refers to molecule B.
[b] Crystal data refer to **7**·CH_2Cl_2.
[c] Identical values for each Ni^{II} atom assumed.
[d] Average values

Table 2 reveals that the tetrazolato complexes **4**-**7** have smaller J_1 values than the pyrazolate complex **2**. This fact might be attributed to the differences in the Ni–$N_{coligand}$ binding strength. The observation that the tetrazolato complex **4** has the longest Ni-N coligand bonds and the smallest J_1 value would be consistent with this in view. Further experiments are planned in order to establish whether this tendency applies as a general rule.

Conclusion

In summary, we presented the synthesis and characterization of a new tetranuclear nickel(II) complex, where two Ni_2 amine-thiophenolate subunits are interconneted by a 5,5'-(1,4-Phenylene)bis-1*H*-tetrazolato bridging ligand. The complex forms discrete complexes in solid state and in solution, as verified by various analytical methods. The magnetic properties of this compound reveal weak ferromagnetic exchange interactions within the dinuclear Ni^{II} subunits. Coupling across the tetrazolato bridge was found to be negligible. The dinuclear Ni^{II}complexes **4** – **6** also reveal weak ferromagnetic exchange interactions between the Ni^{II} (S=1) ions. The magnitude of the exchange interactions appears to decrease with increasing Ni-$N^{heterocycle}$ bond length.

Experimental Section

General remarks: Solvents and reagents were of reagent grade quality and used as received unless otherwise specified. Synthetic steps involving $[Ni^{II}_2L(\mu\text{-}Cl)][ClO_4]$ were carried out under an inert atmosphere of nitrogen. The compounds 5,5'-(1,4-phenylene)bis-1*H*-tetrazole [7], $[Ni^{II}_2L(\mu\text{-}Cl)][ClO_4]$ [6], $[Ni^{II}_2L(HCN_4)][BPh_4]$ [5], $[Ni^{II}_2L(MeCN_4)][BPh_4]$ [5] and $[Ni^{II}_2L(PhCN_4)][BPh_4]$ [5] were prepared according to the literature procedures. Melting points were determined with a Barnstead Electrothermal IA9100 Series instrument in open glass capillaries and are uncorrected. Infrared spectra were recorded on a Bruker Vector27 FT-IR-spectrometer. Electronic absorption spectra were taken on a JASCO V670 UV/vis/near spectrometer, elemental analyses on a VARIO EL – elemental analyzer. Temperature-dependent magnetic susceptibility measurements on powdered solid samples were carried out using a MPMS 7XL SQUID magnetometer (Quantum Design) over the temperature range from 2 – 300 K at an applied magnetic field of 1.0 Tesla. The observed susceptibility data were corrected for underlying diamagnetism.

Safety note! Caution. *Perchlorate salts of transition metal complexes are hazardous and may explode. Only small quantities should be prepared and handled with great care.*

[(Ni^{II}_2L)$_2$(1,4-$(CN_4)_2C_6H_4$)][BPh_4]$_2$ (7). Triethylamine (20 mg, 0.20 mmol) was added to a solution of 5,5'-(1,4-phenylene)bis-1*H*-tetrazole (21 mg, 0.10 mmol) in methanol (30 mL). [Ni^{II}_2L(μ-Cl)][ClO_4] (184 mg, 0.20 mmol) was added to this solution with constant stirring. After the reaction mixture was stirred overnight $LiClO_4 \cdot 3H_2O$ (160 mg, 1.00 mmol) was added. The resulting green precipitate was collected by filtration, washed several times with cold methanol, and redissolved in methanol (70 mL). A solution of $NaBPh_4$ (342 mg, 1.00 mmol) in methanol (50 mL) was added. The mixture was allowed to stir for 1 h, before the volume of the solution was reduced in vacuum to about 50 mL, and the green precipitate was filtered off. The green product was dissolved in CH_2Cl_2 (100 mL) and $NaBPh_4$ (342 mg, 1 mmol) in methanol (20 mL) was added. After removal of CH_2Cl_2 in vacuum, the product was filtered off, washed with ethanol and dried in vacuum to give 155 mg (64 %) of **7** as a green, air-stable, microcrystalline powder. M.p. 358° C (decomp.). IR (KBr, cm^{-1}): ν = 3442 (m), 3054 (s), 3030 (s), 2997 (s), 2964 (vs), 2896 (s), 2863 (s), 2811 (m), 2744 (w), 1636 (w), 1618 (w), 1580 (m), 1479 (s), 1460 (vs), 1426 (s), 1394 (m), 1363 (s), 1308 (m), 1263 (m), 1233 (s), 1200 (m), 1152 (m), 1132 (m), 1109 (w), 1074 (s), 1055 (s), 1041 (s), 999 (m), 982 (w), 930 (m), 911 (m), 881 (m), 843 (w), 825 (s), 817 (s), 807 (m), 749 (s), 733 (vs), 704 (vs), 668 (w), 629 (m), 611 (s), 564 (w), 543 (w), 492 (w), 470 (w), 418 (w). UV/Vis (CH_2Cl_2): $\lambda_{max}(\varepsilon)$= 231 (93852), 270 (63211), 336 (20681), 391 (4889), 447sh (482), 615 (100), 950sh (70), 1133 nm (131 $M^{-1}cm^{-1}$). Elemental analysis (%) for $C_{133}H_{174}B_2Cl_2N_{20}Ni_4S_4$ (2508.50): calcd. C 63.68, H 6.99, N 11.17, S 5.11 found C 63.76, H 7.07, N 10.90, S 5.07. MS (ESI^+, CH_2Cl_2): *m/z* ($\mathbf{7}^{2+}$)=891.36. Single-crystals of **7** suitable for an X-ray structure analysis were

grown by slow diffusion of methanol into a solution of **7** in CH_2Cl_2 or by slow evaporation of an ethanol/acetonitrile solution of **7**.

Crystal structure determination

The X-ray diffraction data were collected at 213 K using a IPDS-I (STOE) diffractometer and graphite monochromated Mo-K_α radiation (λ=0.71073 Å). The intensity data were processed with the program STOE X-AREA [18]. The crystal structure was solved by direct methods and refined by full-matrix least-squares on the basis of all data against F^2 using SHELXL-97 [19]. Non-hydrogen atoms were refined anisotropically whereas the coordinates of the hydrogen atoms were calculated for idealized positions with isotropic displacement parameters.

During refinement **7**·2MeCN was found to contain in summary one acetonitrile molecule per asymmetric unit of which one molecule is only half occupied whereas the other half is additionally disordered on two positions. The DFIX command was used to constrain the bond distances of the acetonitrile molecules to 1.15 Å for the C-N triple bond and 1.50 Å for the C-C distance.

In case of **7**·CH_2Cl_2 the tetraphenyl borate anion was found to be disordered on two positions. Because of this a split atom model for the relevant phenyl groups was introduced using the PART command and the involved carbon atoms were refined isotropically. Electron density attributed to heavily disordered dichloromethane molecules was removed from the structure (and the corresponding F_o) with the SQUEEZE procedure implemented in the PLATON [10] program suite.

Crystal data for **7**·2MeCN: $C_{136}H_{172}B_2N_{22}Ni_4S_4$, M_r = 2499.66, monoclinic, space group

$P2_1/c$, a = 1385.9(1) Å, b = 3021.9(2) Å, c = 1689.5(2) Å, β = 99.00(1)°, V = 6989(1) Å^3, Z = 2, ρ_{calcd} = 1.188 g cm^{-3}; T = –60°C, μ (Mo_{Ka}) = 0.645 mm^{-1} (λ = 0.71073 Å); 33126 reflections measured, 10618 unique, 5648 with $I > 2\sigma(I)$, refinement converged to R_1 = 0.0483, wR_2 = 0.1443 ($I > 2\sigma(I)$), 738 parameters and 6 restraints, min./max. residual electron density = +1.1/ –0.3 e/Å^3.

Crystal data for **7**·CH_2Cl_2: $C_{132}H_{172}B_2N_{20}Ni_4S_4$, M_r = 2423.60, monoclinic, space group $P2_1/n$, a = 1711.38(9) Å, b = 1749.25(7) Å, c = 2491.0(2) Å, β = 108.680(4)°, V = 7064.3(6) Å^3, Z = 2, ρ_{calcd} = 1.139 g cm^{-3}; T = –60°C, μ (Mo_{Ka}) = 0.635 mm^{-1} (λ = 0.71073 Å); 29958 reflections measured, 12280 unique, 9929 with $I > 2\sigma(I)$, refinement converged to R_1 = 0.0405, wR_2 = 0.1268 ($I > 2\sigma(I)$), 729 parameters, min./max. residual electron density = +0.5/ –0.3 e/Å^3.

CCDC 764855-764856 contain the supplementary crystallographic data for this paper. These data can be obtained free of charge from The Cambridge Crystallographic Data Centre via www.ccdc.cam.ac.uk/data_request/cif.

Acknowledgements

We are grateful to Prof. Dr. H. Krautscheid for providing facilities for X-ray crystallographic measurements. This work was supported by the *Deutsche Forschungsgemeinschaft* (Priority programme "Molecular Magnetism", KE 585/4-3), and the University of Leipzig. J. Lach thanks the SAB for an ESF grant.

[1] L. Yet, Pyrazoles, in: A. R. Katritzky, C. A. Ramsden, E. F. V. Scriven, R. J. K. Taylor, V. V. Zhdankin (Eds.), *Comprehensive Heterocyclic Chemistry* III, vol. 4,

Elsevier, Oxford, Tokyo, **2008**, pp. 1–141.

[2] P. N. Gaponik, S. V. Voitekhovich, O. A. Ivashkevich, *Russ. Chem. Rev.* **2006**, *75*, 507–539.

[3] J. Hausmann, V. Lozan, M. H. Klingele, G. Steinfeld, D. Siebert, Y. Journaux, J. J. Girerd, B. Kersting, *Chem. Eur. J.* **2004**, *10,* 1716–1728.

[4] V. Lozan, P. Solntsev, K. V. Domasevitch, B. Kersting, *Eur. J. Inorg. Chem.* **2007**, 3217–3226.

[5] V. Lozan, S. V. Voitekhovich, P. N. Gaponik, O. A. Ivashkevich, B. Kersting, *Z. Naturforsch.* **2008**, *63b*, 496–502.

[6] (a) B. Kersting, G. Steinfeld, *Chem. Commun.* **2001**, 1376–1377; (b) M. H. Klingele, G. Steinfeld, B. Kersting, *Z. Naturforsch.* **2001**, *56b*, 901–907; (c) M. H. Klingele, B. Kersting, *Z. Naturforsch.* **2001**, *56b*, 437–439.

[7] W. G. Finnegan, R. A. Henry, R. Lofquist, *J. Am. Chem. Soc.* **1958**, *80*, 3908–3911.

[8] The $^3A_{2g} \rightarrow {}^3T_{1g}$ (P) transition is presumably obscured by the strong LMCT transitions.

[9] V. Lozan, B. Kersting, *Inorg. Chem.* **2008**, *47*, 5386–5393.

[10] PLATON/SQUEEZE, A. L. Spek, *J. Appl. Cryst.* **2003**, *36*, 7–13.

[11] E. A. Meyer, R. K. Castellano, F. Diederich, *Angew. Chem.* **2003**, *115*, 1244–1287; *Angew. Chem. Int. Ed.* **2003**, *42*, 1210–1250.

[12] Coordinates of the centroid of the central phenyl ring: X1a: 0, 0, 0.

[13] X. He, B. L. An, M. X. Li, *Acta Crystallogr.* **2008**, *E64*, o40.

[14] Z. J. Ma, J. Tao, R. B. Huang, L. S. Zheng, *Acta Crystallogr.* **2005**, *E61*, m361–m363.

[15] V. Lozan, C. Loose, J. Kortus, B. Kersting, *Coord. Chem Rev*. **2009**, *253*, 2244–2260.

[16] julX, E. Bill, http://ewww.mpi-muelheim.mpg.de/bac/logins/bill/julX_en.php.

[17] K. K. Nanda, A. W. Addison, N. Paterson, E. Sinn, L. K. Thompson, U. Sakaguchi, *Inorg. Chem.* **1998**, *37*, 1028–1036.

[18] X-AREA, Stoe & Cie (2006), Darmstadt, Germany.

[19] G. M. Sheldrick, *Acta Cryst.* **2008**, *A64*, 112–122.

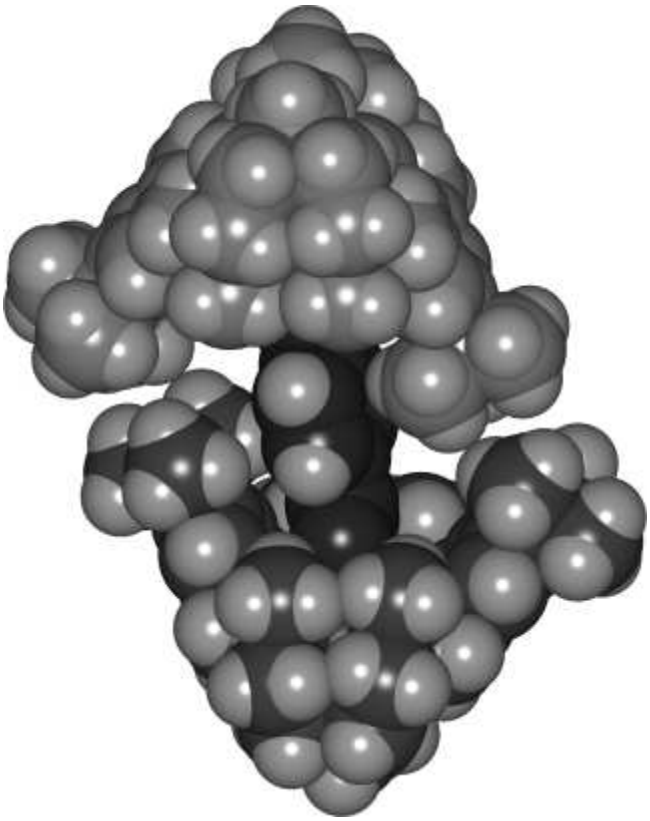

27x34mm (300 x 300 DPI)

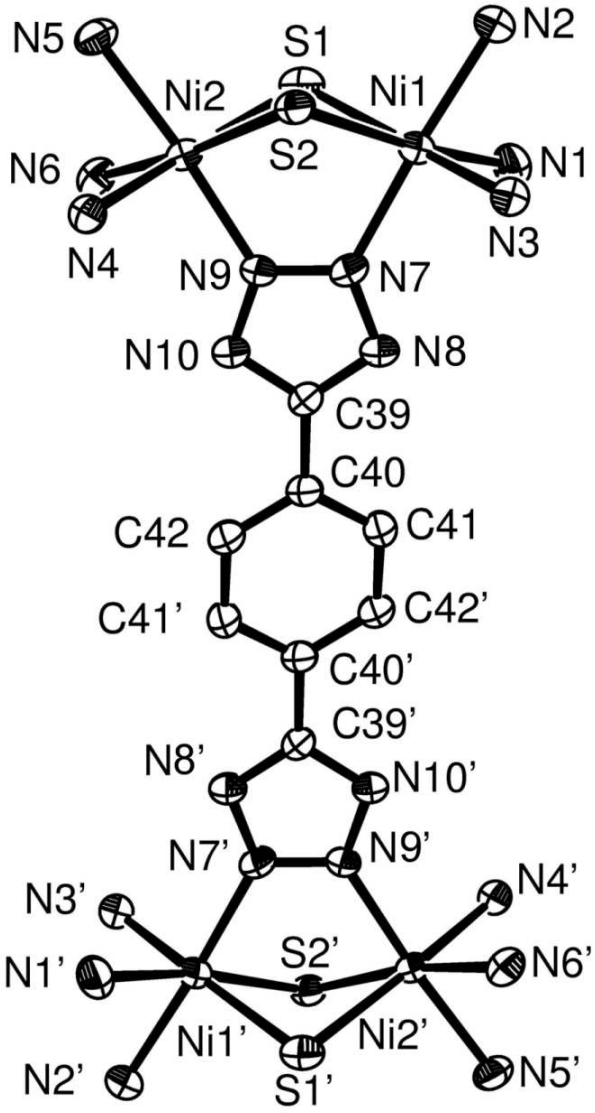

62x112mm (300 x 300 DPI)

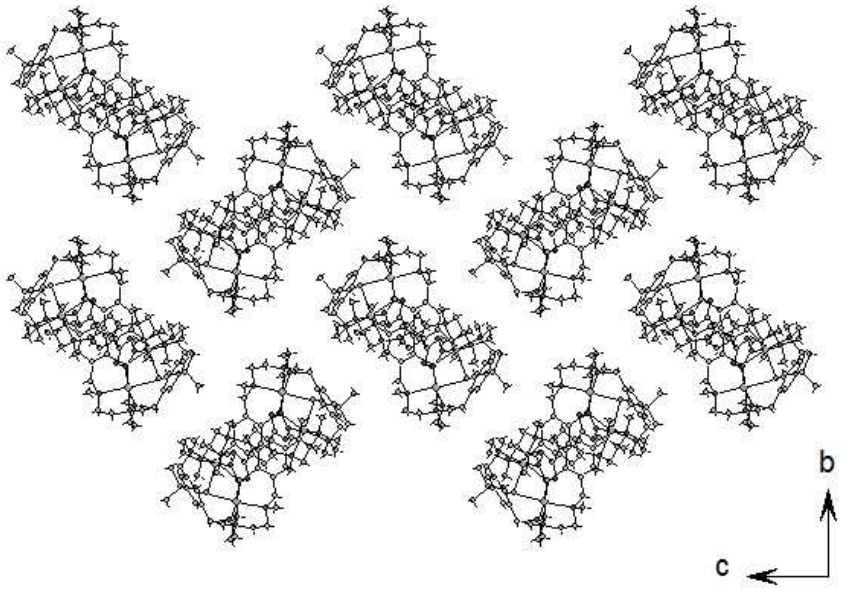

55x46mm (300 x 300 DPI)

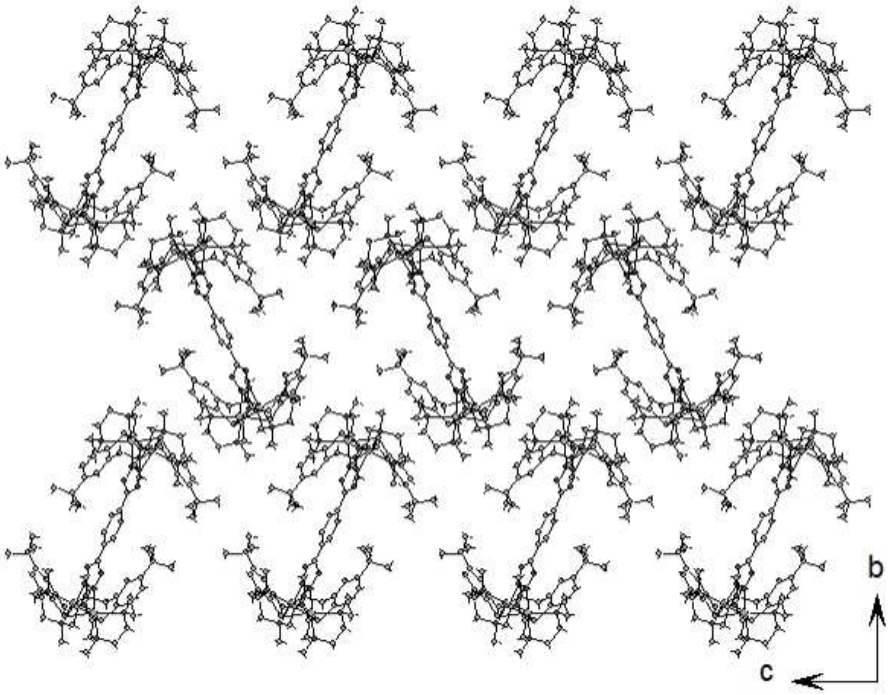

55x46mm (300 x 300 DPI)

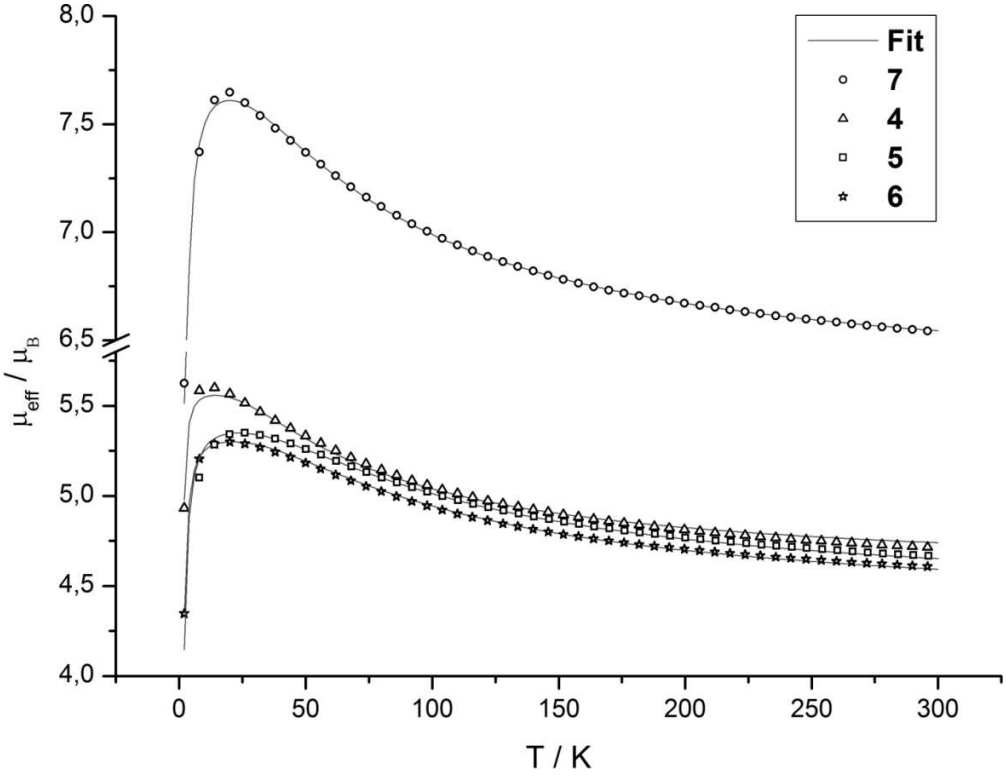

99x76mm (300 x 300 DPI)